Colloids and Surfaces B: Biointerfaces 112 (2013) 380–386

Contents lists available at ScienceDirect

Colloids and Surfaces B: Biointerfaces

journal homepage: www.elsevier.com/locate/colsurfb

Synthesis and characterization of jacalin-gold nanoparticles conjugates as specific markers for cancer cells

Valeria S. Marangoni, Ieda M. Paino, Valtencir Zucolotto*

Physics Institute of São Carlos, University of São Paulo, São Carlos, BR-13560970, Brazil

ARTICLE INFO

Article history:
Received 17 May 2013
Received in revised form 4 July 2013
Accepted 16 July 2013
Available online xxx

Keywords:
Gold Nanoparticles
Jacalin
Nanobiocomposites
Nanomedicine

ABSTRACT

New nanobiocomposites that combine nanoparticles and biomolecules have been shown very relevant for medical applications. Recently, cancer diagnostics and treatment have benefited from the development of nanobiocomposites, in which metallic or magnetic nanoparticles are conjugated with specific biomolecules for selective cell uptake. Despite recent advances in this area, the biomedical applications of these materials are still limited by the low efficiency of functionalization, low stability, among other factors. In this study, we report the synthesis of jacalin-conjugated gold nanoparticles, a nanoconjugate with potential application in medical areas, especially for cancer diagnosis. Jacalin is a lectin protein and it was employed due to its ability to recognize the Galβ1-3GalNAc disaccharide, which is highly expressed in tumor cells. Gold nanoparticles (AuNPs) were synthesized in the presence of generation 4 polyamidoamine dendrimer (PAMAM G4) and conjugated with fluorescein isothiocyanate (FITC)-labeled jacalin. The AuNPs/jacalin nanoconjugates were characterized by transmission electron microscopy (TEM), dynamic light scattering (DLS) and vibrational spectroscopy (FTIR). We also performed an investigation using isothermal titration calorimetry (ITC) and fluorescence quenching measurements to understand the interactions occurring between the AuNPs and jacalin, which revealed that the nanoconjugate formation is driven by an entropic process with good affinity. Furthermore, *in vitro* tests revealed that the AuNPs/jacalin-FITC nanoconjugates exhibited higher affinity for leukemic K562 cells than for healthy mononuclear blood cells, which could be useful for biomedical applications, including cancer cells imaging.

© 2013 Elsevier B.V. All rights reserved.

1. Introduction

The development of new multifunctional materials with high impact for cancer diagnostics and therapy is a major challenge in medicine. Nanobiocomposites that combine the recognition properties of biomolecules with the electronic, optical and magnetic properties of nanoparticles have been considered strong candidates for biomedical application [1]. For example, nanoparticle-based strategies may incorporate multiple types of molecules onto a single nanoparticle surface, creating nanoconjugates that may perform multiple functions, and thus have provided important advances [2].

Gold nanoparticles (AuNPs), in particular, have attracted attention because of their unique optical and electronic properties, making them useful for many applications as biosensors [3], contrast agents [4], and vehicles for controlled intracellular delivery [5] as well as in cancer detection and treatment [6]. Several strategies have been used to produce gold nanoparticles with high control over size and shape. Among others, poly(amido amine) dendrimers have been used as stabilizing agents in the synthesis of gold nanoparticles with controlled dimensions [7,8].

For applications in cancer detection and treatment, the particles must selectively localize at and incorporate into cancer cells. Nanoparticles may be accumulated in the tumor by a passive targeting by taking advantage of the enhanced permeability and retention effect (EPR effect) [9–11]. On the other hand, the active targeting may be achieved *via* functionalization of the nanoparticle surfaces [11] with specific proteins [12], peptides [13], aptamers [14] and antibodies [15]. Therefore, conjugating biomolecules to gold nanoparticles may provide nanomaterials with additional interaction capabilities [16].

A variety of methods have been used to produce protein-functionalized nanoparticles. These methods include electrostatic adsorption, chemisorption of thiol derivatives, covalent binding through bifunctional linkers and specific affinity interactions [1,16]. As an example of the last method, streptavidin-functionalized gold nanoparticles have been used for the affinity binding of

* Corresponding author at: Physics Institute of São Carlos, University of São Paulo, Avenida Trabalhador Sãocarlense, 400, CEP: 13560-970 São Carlos, São Paulo, Brazil. Tel.: +55 16 3373 9875.
E-mail address: zuco@ifsc.usp.br (V. Zucolotto).

0927-7765/$ – see front matter © 2013 Elsevier B.V. All rights reserved.
http://dx.doi.org/10.1016/j.colsurfb.2013.07.070

biotinylated proteins (*e.g.*, immunoglobulins and serum albumins) [17]. Nevertheless, despite recent advances in the development of nanobiocomposites, the application of these materials to medicine has been limited by the incomplete understanding of the interactions between nanomaterials and biomolecules and by experimental factors including the low efficiency of functionalization, low stability and high toxicity of nanoparticles.

Aberrant glycosylation has been observed in all types of human cancers and many glycosyl epitopes constitute tumor-associated antigens [18]. Due the capability to bind specifically and reversibly to mono- and oligosaccharides [19], lectins may be used as cancer targeting upon conjugation with nanoparticles [20–23]. However, the synthesis and applications of lectins conjugated with gold nanoparticles are little explored so far.

Jacalin is a lectin from jackfruit seeds that has a molecular weight of 66,000 g mol^{-1} and forms a tetramer at neutral pH [24]. This protein may specifically recognize a tumor-associated T-antigenic disaccharide Galβ1-3GalNAc [24–27], overexpressed in more than 85% of human carcinomas, including breast, colon, bladder, cavity and prostate [26].

In this study, we describe the development and a detailed characterization of jacalin-gold nanoparticle conjugates, aimed at understanding the interactions occurring between the protein and AuNPs. Furthermore, *in vitro* tests in culture cells were performed to evaluate the capability of the new nanoconjugated in target cancer cells.

2. Experimental

2.1. Materials

All reagents were used as received, and all solutions were prepared with Milli-Q water (18.2 MΩ cm^{-1}) from a Millipore system. Tetrachloroauric acid ($HAuCl_4$), generation 4.0 PAMAM dendrimers (PAMAM G4), formic acid and fluorescein isothiocyanate (FITC) were acquired from Sigma–Aldrich. Buffer solutions were prepared using sodium phosphate monobasic and sodium phosphate dibasic from Sigma–Aldrich and sodium chloride from J.T. Baker.

2.2. Synthesis of gold nanoparticles stabilized by PAMAM-G4

Generation 4 dendrimers were chosen for their ability to form small and highly stabilized particles in aqueous medium [7,8]. Nanoparticles may be encapsulated into the cavities of PAMAM or stabilized by several PAMAM molecules. In the former, dendrimer-encapsulated AuNPs with diameters of less than 4 nm may be obtained by a fast reduction process using $NaBH_4$ [8]. In contrast, a reduction by a weak reducing agent can yield larger nanoparticles that may be useful in cellular labeling and imaging studies [28]. In this study, we used formic acid as reducing agent to promote a slow reduction of the nanoparticles. The synthesis started by mixing equal volumes of $HAuCl_4$ (1.0 mmol L^{-1}) and PAMAM G4 (0.7 mmol L^{-1}) and then a solution of formic acid 10% v/v. The system was stirred for 30 min at room temperature and protected from light. Following, it was removed from stirrer and kept for four hours at room temperature, protected from light.

The average number of Au atoms (N) in the each AuNP was estimated according to [29]. We assumed spherical particles with average diameter of about 6.1 nm obtained from TEM (see Supplementary Material). This result was used to estimate the molar concentration of the AuNPs suspension [29] for using in fluorescence quenching analysis and ITC.

3. Purification of jacalin

The jacalin protein was obtained from the crude extract derived from seeds of *Artocarpus integrifolia* (jackfruit). The seeds were washed in Milli-Q water, crushed and resuspended in PBS buffer (pH = 7.4). This mixture was stirred for 12 h at 4 °C and centrifuged at 4000 rpm. The supernatant was separated and purified by affinity chromatography using a Sepharose D-galactose-immobilized resin. The other proteins were eluted in PBS buffer, and jacalin was eluted in PBS buffer containing D-galactose (0.2 mol L^{-1}). This fraction was purified again using molecular exclusion chromatography. Volumes of 1 mL were added to a Superdex75 3.2/30 (Pharmacia Biotech Smart System) column coupled to an Äkta purifier system (GE Healthcare) in PBS buffer. The flow was 0.5 ml min^{-1}, and the absorbance was monitored at 220 and 280 nm. The purity was checked using polyacrylamide gel electrophoresis. The mass concentration of Jacalin was estimated by measuring the absorbance at 280 nm and using ε_{280} = 1.14 cm^2 mg^{-1} and the molecular mass of 66,000 Da, which corresponds to four carbohydrate-binding sites [30]. Jacalin was further labeled with fluorescein (FITC) by adding a FITC solution (1.0 mg mL^{-1}) to a jacalin solution (1.0 mg mL^{-1}) at pH ~8.0. The system was stirred and protected from light for one hour at room temperature and more two hours at 4 °C. The excess FITC was eliminated using dialysis against PBS buffer pH = 7.4 with a 25 kDa membrane (Spectra/Por) at 4 °C. The ratio of FITC to protein was estimated by measuring the absorbance at 495 nm and 280 nm according to Beer-Lambert law.

3.1. Preparation of AuNPs/jacalin nanoconjugates

The AuNPs/jacalin nanoconjugate was prepared by adding 300 μL of AuNPs (about 5 mg mL^{-1}) to 1.3 mL of 0.6 mg mL^{-1} jacalin or jacalin-FITC. The system was gently stirred at 4 °C and protected from light for 24 h. Free jacalin was separated with centrifugation at 13,000 rpm and 4 °C for 15 min using a Centrifuge 5415 R (Eppendorf). The precipitated was suspended in phosphate buffer (10 mmol L^{-1}, pH = 7.4).

4. Characterization

Transmission electron microscopy (TEM) images were obtained using a JEOL/JEM-2100 transmission electron microscope (200 kV). One drop of each of the diluted samples was deposited on a carbon film copper grid 300 mesh (Ted Pella, Inc.) and dried at room temperature.

UV–vis spectra experiments were carried out on a Hitachi U-2900 spectrometer using a 1 cm quartz cell. Circular dichroism (CD) spectra were measured using a Jasco-720 spectropolarimeter with a 0.1 cm quartz cell. The CD spectra were recorded from 190 to 250 nm. The CD spectra of AuNPs and of the buffer were also measured and subtracted from nanoconjugate. The secondary structures, such as α helix, β sheet, turn and unordered, of pure jacalin and the AuNPs/jacalin nanoconjugates were calculated from the CD data using the CONTIN/LL (CD-pro) program.

Dynamic light scattering (DLS) has been extensively used to measure the *in situ* size distribution in nanoparticles suspension. The analyses were performed in triplicate at 25 °C using a Malvern Nano-ZS spectrometer (Malvern Instruments, UK).

Fourier transform infrared spectroscopy (FTIR) was used to identify the molecular groups involved in the interaction between the AuNPs and the protein. The samples were lyophilized and compressed with KBr. The FTIR spectra were obtained in a Thermo Nicolet 6700 Spectrophotometer with a resolution of 4 cm^{-1} in the transmittance mode.

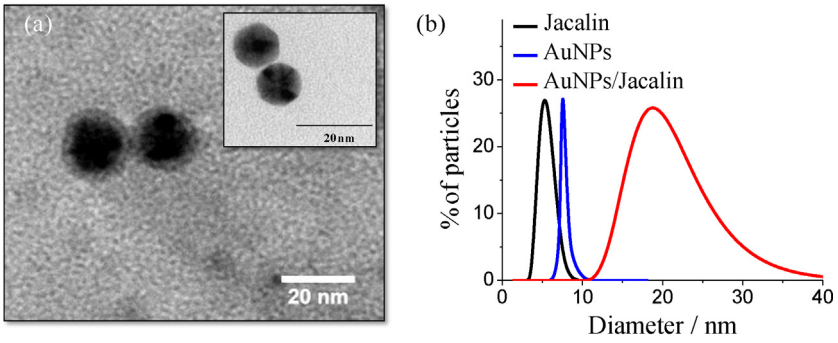

Fig. 1. (a) TEM image of AuNPs before (inset) and after conjugation with jacalin and (b) DLS measurements for free jacalin, AuNPs and AuNPs/jacalin nanoconjugate.

Fluorescence spectroscopy was used to measure the quenching of the fluorescence from tryptophan and tyrosine upon the binding of jacalin to the AuNPs. Different concentrations of AuNPs were added to the jacalin (0.7 mg mL^{-1}) solution. The spectra were collected from 295 to 500 nm in a quartz cell using a ISS-K2 fluorometer (Illinois, USA) upon an excitation wavelength of 280 nm. The data were analyzed using the Stern–Volmer and modified Stern–Volmer equations [31].

Isothermal titration calorimetry (ITC) was utilized to investigate the thermodynamic parameters of the interaction between jacalin and AuNPs [32]. The measurements were performed in a VP-ITC Microcal microcalorimeter at 25 °C. AuNPs and jacalin were dialyzed against phosphate buffer (10 mmol L^{-1}, pH = 7.4). AuNPs (0.047 μmol L^{-1}) was titrated in constant volumes of 9 μL on a cell containing 1.47 mL of jacalin (10 μmol L^{-1}), and the cell was stirred at 255 rpm. A higher concentration of AuNPs was impossible to be used due their low stability in this pH. The reference cell was filled with 1.47 mL of Milli-Q water for all experiments. The heat of dilution was determined by titrating the AuNPs on phosphate buffer and subtracted from the experimental titration data.

5. Cell culture

Tests in cell cultures were performed to investigate the interaction of AuNPs/jacalin-FITC nanoconjugates with human leukemia (K562) and healthy mononuclear cells. All reagents were autoclaved beforehand to avoid contamination, and the experiments were performed in a laminar flow cabinet. The K562 cells (1×10^5 cells/mL) were incubated in RPMI culture media supplemented with 10% with fetal bovine serum (FBS), 0.06 g L^{-1} of penicillin and 0.1 g L^{-1} of streptomycin in a stove at 37 °C with 5% CO_2. The cellular growth was monitored using a Nikon Eclipse TS 100 inverted microscope (Japan).

Peripheral blood mononuclear cells (PBMCs) were collected from healthy adult female and male volunteers, excluding pregnant women and tobacco or medication users. The subjects were informed of all the legal procedures. The study was approved by the Ethics Committee of the Federal University of São Carlos in accordance with the principles in the Declaration of Helsinki. Mononuclear cells were isolated using Ficoll-Hypaque 1077 (Histopaque, Sigma–Aldrich) fractionation. The PBMCs were collected carefully, washed in PBS twice (240 × *g* for 10 min), and suspended in RPMI 1640 medium with 10% FBS. The individual PBMC-derived cultures were acquired from separate volunteers at different times. Cells viability was investigated immediately before all the assays (data not shown), showing viability higher than 95% according to the trypan blue (Sigma–Aldrich®, USA) exclusion assay.

5.1. Incubation of the cells with the nanoconjugate

The cells were incubated in microplate cultures in a final volume of 500 μL and were treated with 1.0 μmol L^{-1} of free jacalin-FITC and AuNPs/jacalin-FITC. The concentration was based on the protein concentration in all cases measuring by the absorbance at 280 nm. After 3 h of incubation, the cells were washed two times with sterile PBS buffer by centrifugation, and images were obtained using a Nikon Eclipse TS 100 fluorescence microscope coupled with a Nikon DS-Ri1 digital camera and a 40× objective.

6. Results and discussion

Fig. 1a shows a TEM image of AuNPs before (inset) and after the conjugation with jacalin-FITC. In contrast to AuNPs, the AuNPs/jacalin-FITC nanoconjugate presented a shadow around the particle surface, which may be an indicative of the formation of a protein layer around the AuNPs. This phenomenon has been observed by other authors in the study of protein-conjugated nanoparticles [12,33,34].

The DLS measurements (Fig. 1b) also revealed a significant increase in size compared with that of the free jacalin and AuNPs. This increased size in the nanoconjugate may be associated with the conjugation of protein on the nanoparticle surface. The thickness of this protein shell on the AuNPs surface is approximately 3.2 nm based on the TEM images and is smaller than the thickness expected from the DLS analyses (about 6.1 nm), which measure the hydrodynamic diameter. This decrease has also been described to be a result of drying and subjecting the sample to a high-vacuum and high-energy electron beam on the TEM images [33].

Fig. 2a displays the UV–vis spectra of jacalin, AuNPs and AuNPs/jacalin. The individual spectral features of jacalin and the nanoparticles appear in the spectrum of the nanoconjugate at approximately 280 and 523 nm, respectively, even after washing. It is possible to observe a slightly red shift on the AuNPs band compared with its individual spectra, which may be indicative of its surface modification [12]. The AuNPs/jacalin nanoconjugated also presented higher stability at neutral pH than free AuNPs. AuNPs precipitated after 24 h at neutral pH, while the AuNPs/jacalin nanoconjugate was stable for several months (data not shown).

The inset of Fig. 2a shows the spectra of jacalin-FITC and AuNPs/jacalin-FITC. The spectra shows the FITC absorbance peak at about 490 nm and Fig. 2b shows its emission band at 518 nm, which overlaps with the AuNPs surface plasmon band at 523 nm. In this way, it should be expected an effective quenching of FITC fluorescence due the presence of the AuNPs. However, as we can see at Fig. 2b, it is still possible to observe a considerable FITC fluorescence in the AuNPs/jacalin-FITC conjugates. Further, the fluorescence microscopy images, shown in Fig. 7, presented good fluorescence

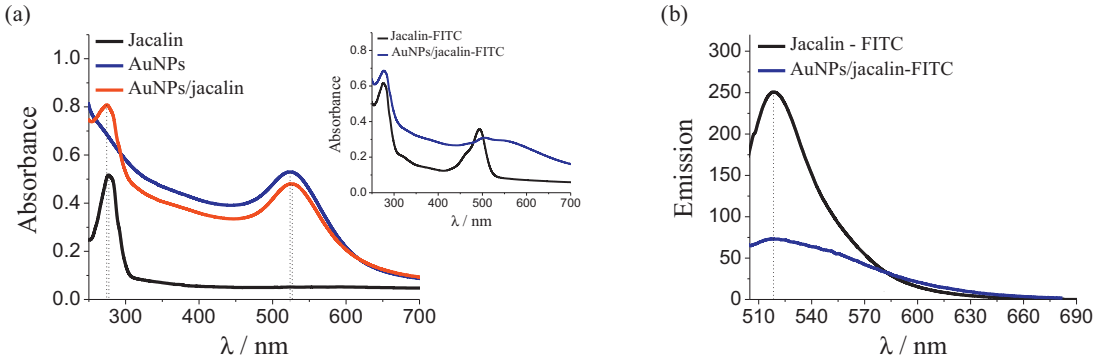

Fig. 2. (a) UV–vis spectra of AuNPs, jacalin and AuNPs/jacalin conjugate and the inset shows the spectra of free jacalin labeled with FITC and AuNPs/jacalin-FITC. (b) Emission spectra for jacalin-FITC and AuNPs/jacalin-FITC at about the same concentration of jacalin.

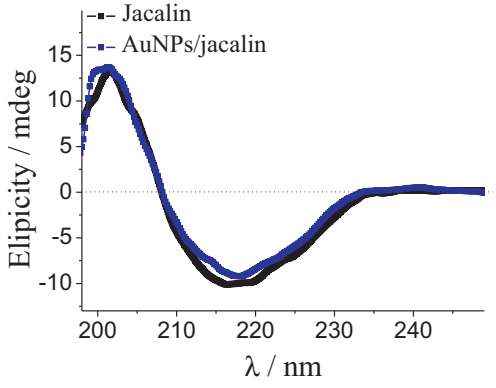

Fig. 3. CD spectra of free jacalin and the AuNPs/jacalin nanoconjugate.

when excited with 488 nm. This behavior was also observed by Shukla et al. [35]. The authors showed that AuNP/Lysine-FITC and AuNP/Poly-Lysine-FITC conjugates when excited with 488 nm argon laser showed considerably stable fluorescence and excellent confocal miscrocopy images. In contrast, FITC conjugated directly with AuNPs showed no fluorescence [35]. These observations suggest that the addition of spacer groups between AuNPs and FITC could avoid energy transference and rapid quenching of fluorescence emission from FITC [35].

For targeting properties of the nanoconjugate it is important that the protein keeps its structure and function. CD was used to investigate the secondary structure of the protein in the AuNPs/jacalin nanoconjugate. Fig. 3 shows the spectra of free jacalin (black line) and AuNPs/jacalin (blue line). Both indicate a typical β sheet spectrum. The deconvolution of the spectra was performed using the CONTINLL (CD/Pro Package) program [36]. The data (Table 1) suggest that there was no significant modification in the protein structure percentages and indicate that the protein maintained its secondary structure even after conjugation with the nanoparticles, what is important for biological applications.

FTIR analysis may provide important information about the groups involved in the interaction between nanoparticles and proteins [37]. The FTIR spectra of AuNPs, jacalin and AuNPs/jacalin are shown in Figure 4. The bands in the AuNPs spectrum are from the PAMAM G4 dendrimer. The strong bands at 1651 and 1594 cm^{-1} correspond to the C=O stretch, N—H deformation, and C—N stretch. The main bands from jacalin are the vibrational mode of the amide groups [38]. The amide I vibration (about 1630 cm^{-1}) arises mainly from the C=O stretching vibration, and the amide II mode is mainly the out-of-phase combination of the N—H in-plane bend and the C—N stretching vibration.Given the complexity of the spectra because the overlapping of some bands, the accurate analysis is difficult. Nevertheless, it can be inferred that the nanoconjugate contains the main bands from AuNPs and jacalin. Additionally, the bands from jacalin below 1300 cm^{-1} are more intense than those from free jacalin. Most of these bands are assigned to the vibration mode of the COO^- or COOH and C—O groups of amino acid side chains, mainly glutamic acid, aspartic acid, serine and tyrosine [39], which compose approximately 25% of the primary structure of jacalin. Therefore, these changes may be related to the interactions between these groups with the amino groups from PAMAM.

Table 1
Percentages of secondary structures of free jacalin and the AuNPs/jacalin nanoconjugate (CONTINLL CD/Pro Package).

	α helix	β sheet	turns	unrd
Jacalin	3.7%	42.9%	20.9%	32.5%
AuNP/jacalin	3.5%	41.7%	20.7%	34.1%

The fluorescence of the aromatic amino acids in proteins is sensitive to the environment, and the fluorescence spectra may provide information about the interaction between the protein and the nanoparticles [40]. Therefore, the emission spectra of jacalin were obtained in the absence and presence of different concentrations of AuNPs (Fig. 5a). A plot of the fluorescence intensity at 325 nm *vs.* concentration is shown in the inset of Fig. 5a. Increasing the concentration of AuNPs resulted in quenched jacalin fluorescence, followed by stabilization. Quenching of protein fluorescence by gold nanoparticles has been reported earlier [40]. The data were analyzed using the Stern–Volmer equation [31,40]:

$$\frac{F_0}{F} = 1 + K_{SV}[\text{AuNPs}] \quad (1)$$

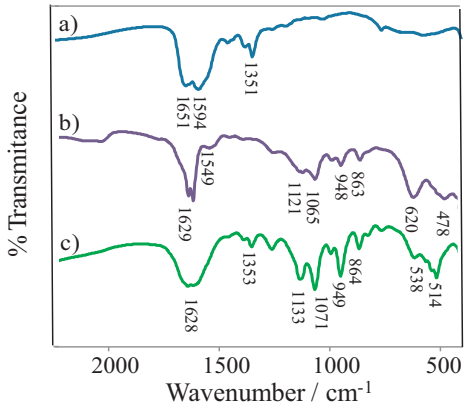

Fig. 4. Infrared spectroscopy of (a) AuNPs; (b) Jacalin and (c) AuNPs/jacalin.

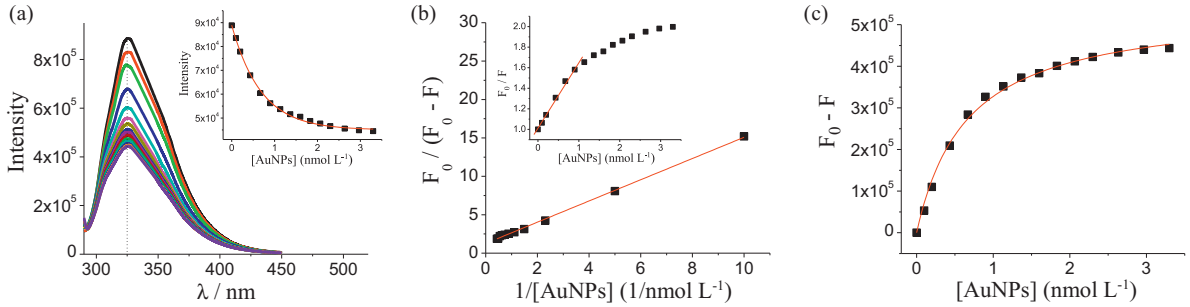

Fig. 5. (a) The fluorescence quenching spectra of jacalin at different concentration of AuNPs and (inset) fluorescence intensity at 325 nm as function of the AuNP concentration; (b) Modified Stern–Volmer plots and (inset) Stern–Volmer plot showing the deviation from linearity; (c) Determination of K_a using the quenching of fluorescence. The line represents a Langmuir-based model.

where F_0 and F are the fluorescence intensities before and after the addition of the quencher, respectively, K_{SV} is the Stern–Volmer quenching constant and [AuNPs] is the concentration of the gold nanoparticles. A linear Stern–Volmer plot is indicative of a single class of fluorophores, all equally accessible to the quencher [31,41]. The plot of the F_0/F against [AuNPs] is shown in the inset of Fig. 5b and reveals that there are at least two populations of fluorophore. Moreover, the stabilization at non-zero values suggests the existence of a fluorophore that is not accessible to the quenching. The fraction of the fluorophore accessible to the quencher was assessed using the modified Stern–Volmer equation [31]:

$$\frac{F_0}{F_0 - F} = \frac{1}{f_a \times K_{SVa} \times [AuNPs]} + \frac{1}{f_a} \quad (2)$$

where f_a is the fraction of fluorophore-sites accessible to the quencher and K_{SVa} is the Stern–Volmer quenching constant of the accessible fraction. The plot in Fig. 5b is linear, and the fit gives $f_a = 0.79$, which indicates that approximately 79% of the fluorophores are accessible. The value of K_{SVa} is approximately $9.1 \times 10^9\ M^{-1}$ and suggests that the quenching of the fluorescence occurs by a specific interaction between AuNPs and jacalin, ie, by a mechanism in which a complex is formed [31,40]. The affinity constant was determined using a Langmuir-type model, assuming one affinity-class binding sites [41].

$$F_0 - F = \frac{(F_0 - F)[\text{AuNPs}]}{\frac{1}{K_a} + [\text{AuNPs}]} \quad (3)$$

where F_∞ is the fluorescence intensity when the protein is saturated with the quencher. The plot in Fig. 5c gives an affinity constant of approximately $1.5 \times 10^9\ M^{-1}$, which was compared to the ITC results.

ITC has become a very useful technique to evaluate the thermodynamic parameters of the interaction between nanoparticles and biomolecules [42,43]. Fig. 6 shows the heats of each titration of AuNPs into calorimetric cell containing jacalin. As the injections proceeds, the number of binding sites decreases continuously until saturation and the endothermic calorimetric response becomes constant. The data from the integrated area of each peak were adjusted according to the one-site model to determine the binding stoichiometry and thermodynamic parameters. It is noteworthy that these parameters were calculated based on the estimated molar concentration of the AuNPs and then they were used just as a qualitative study. Based on the ITC data, a number of 10 protein molecules per nanoparticle was estimated, and the affinity constant K_a was found to be at the same order of magnitude as the value obtained from the fluorescence quenching analyses. Furthermore, the unfavorable endothermic process was compensated by a positive change in entropy, resulting in a favorable Gibbs free energy. This effect probably arise from release of numerous bound water from protein and AuNPs surfaces, which results in unfavorable enthalpy changes, but high favorable entropy changes that contribute to the complex stability [44].

Entropic driven processes have been observed in different protein-nanoparticle systems. For example, the electrostatic interactions between β-lactoglobulin and cationic gold nanoparticles described by Chen et al. [45]. Also, De et al. [44] showed that the complexation between green fluorescence protein (GFP) and bovine serum albumin (BSA) with cationic gold nanoparticles involves unfavorable enthalpy change and a favorable entropy gain. However, the interaction of the nanoparticles with acid phosphatase (PhosA) is exothermic with an unfavorable entropy loss. The authors explained that in the complexation with smaller proteins like GFP (27 kDa) and BSA (66.3 kDa), there are higher degree of surface interaction that results from the release of large amount of water of hydration from interface [44]. Jacalin has a similar molecular weight to BSA and this effect should also play one of the main roles in the AuNPs–jacalin conjugation.

It is known that jacalin may induce differentiation of leukemic cell K562 [46], which has been attributed to be mediated by the recognition of T-antigenic [47]. In this way, *in vitro* tests in cell cultures were performed to evaluate the ability of the AuNPs/jacalin-FITC nanoconjugates to specifically interact with K562 leukemic cells. The stability of the nanoconjugates in cell culture media was evaluated by DLS [48] and the results revealed no significant modification in the average diameter of the nanoconjugates even for long periods of incubation (Supplementary Material).

The microscopy images (Fig. 7) show that after 3 h of incubation the AuNPs/jacalin-FITC nanoconjugates adhered to human K562 leukemia cells (Fig. 7a and b) but not to healthy mononuclear blood cells (Fig. 7c and d). Control experiments with jacalin-FITC

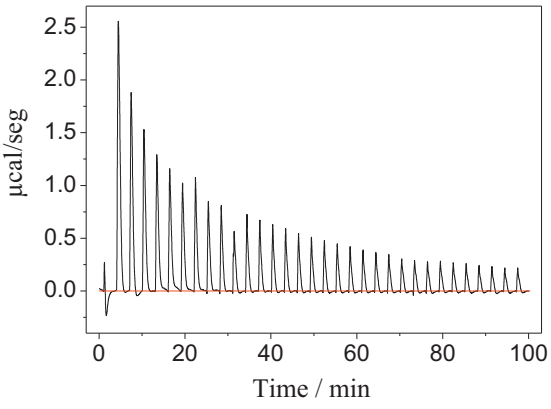

Fig. 6. ITC data from the titration of AuNPs into calorimetric cell containing jacalin at 25 °C.

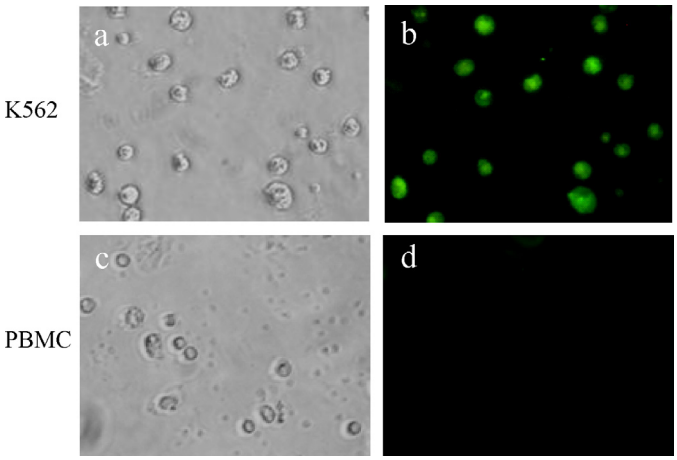

Fig. 7. Optical microscopy (a and c) and its respective fluorescence images (b and d) obtained with a 40× objective after 3 h of incubation with AuNPs/jacalin-FITC and washing two times with PBS buffer of (a and b) K562 cells and (c and d) PBMCs.

conjugates (with no AuNPs), also revealed fluorescence only for K562 cells (data not shown). This behavior was also observed by Chatterjee et al. to ALA (*Artocarpus lakoocha* agglutinin), a jacalin like lectin, conjugated with quantum dots [49]. This specificity may be relevant for the development of new specific cancer agents.

Cytotoxicity assays using the MTT method were performed for all nanoparticles system employed here, and none significant toxicity was observed of the AuNPs/jacalin nanoconjugates against healthy L929 cells. For example, the AuNP/jacalin conjugates exhibited no significant toxicity against L929 cells at concentrations of 0.5 $\mu mol\,L^{-1}$. For higher concentrations, *viz.*, 1.0 $\mu mol\,L^{-1}$, a cell viability higher than 85% was observed even after 24 h of incubation with AuNps/jacalin nanoconjugates, which was lower than that exhibited by gold nanoparticles (see Supplementary Material).

7. Conclusions

We presented a detailed study of the interactions between AuNPs and jacalin, a nanoconjugate with potential for cancer applications. Jacalin was efficiently conjugated with PAMAM G4 stabilized gold nanoparticles, as showed in the TEM images, DLS and UV–vis spectroscopy. The calorimetric study allowed a better understanding of the interactions occurring between the protein and the nanoparticles, revealing an entropy-driven conjugation with good affinity, consistent with the fluorescence quenching measurements. The protein maintained its secondary structure upon conjugation with AuNPs, and *in vitro* tests revealed that the AuNPs/jacalin-FITC nanoconjugates had higher affinity for human leukemia cells (K562) than for healthy mononuclear blood cells. The interactions between nanoparticles and biomolecules play one of the main roles for the development of new nanocomposites for medical applications. Besides the development of a new composite with potential for cancer applications, the results presented here are also useful for a better understanding of the nano-bio interface and in the development of enhanced systems with high stability and multiple properties for nanomedicine.

Acknowledgement

The authors thank LME/LNNano for technical support during the electron microscopy and FAPESP for financial support.

Appendix A. Supplementary data

Supplementary data associated with this article can be found, in the online version, at http://dx.doi.org/10.1016/j.colsurfb.2013.07.070.

References

[1] E. Katz, I. Willner, Integrated nanoparticle-biomolecule hybrid systems: synthesis, properties, and applications, Angew Chem. Int. Ed. 43 (2004) 6042–6108.
[2] R. Bardhan, S. Lal, A. Joshi, N.J. Halas, Theranostic nanoshells: from probe design to imaging and treatment of cancer, Acc. Chem. Res. 44 (2011) 936–946.
[3] L. He, M.D. Musick, S.R. Nicewarner, F.G. Salinas, S.J. Benkovic, M.J. Natan, C.D. Keating, Colloidal Au-enhanced surface plasmon resonance for ultrasensitive detection of DNA hybridization, J. Am. Chem. Soc. 122 (2000) 9071–9077.
[4] J. Roth, The silver anniversary of gold: 25 years of the colloidal gold marker system for immunocytochemistry and histochemistry, Histochem. Cell Biol. 106 (1996) 1–8.
[5] P. Ghosh, G. Han, M. De, C.K. Kim, V.M. Rotello, Gold nanoparticles in delivery applications, Adv. Drug Deliv. Rev. 60 (2008) 1307–1315.
[6] J.A. Barreto, W. O'Malley, M. Kubeil, B. Graham, H. Stephan, L. Spiccia, Nanomaterials: applications in cancer imaging and therapy, Adv. Mater. 23 (2011) H18–H40.
[7] R.M. Crooks, M.Q. Zhao, L. Sun, V. Chechik, L.K. Yeung, Dendrimer-encapsulated metal nanoparticles: synthesis, characterization, and applications to catalysis, Acc. Chem. Res. 34 (2001) 181–190.
[8] K. Esumi, A. Suzuki, A. Yamahira, K. Torigoe, Role of poly(amidoamine) dendrimers for preparing nanoparticles of gold, platinum, and silver, Langmuir 16 (2000) 2604–2608.
[9] H. Maeda, J. Fang, T. Inutsuka, Y. Kitamoto, Vascular permeability enhancement in solid tumor: various factors, mechanisms involved and its implications, Int. Immunopharmacol. 3 (2003) 319–328.
[10] H. Maeda, G.Y. Bharate, J. Daruwalla, Polymeric drugs for efficient tumor-targeted drug delivery based on EPR-effect, Eur. J. Pharm. Biopharm. 71 (2009) 409–419.
[11] L. Brannon-Peppas, J.O. Blanchette, Nanoparticle and targeted systems for cancer therapy, Adv. Drug Deliv. Rev. 56 (2004) 1649–1659.
[12] T.H.L. Nghiem, T.H. La, X.H. Vu, V.H. Chu, T.H. Nguyen, Q.H. Le, E. Fort, Q.H. Do, H.N. Tran, Synthesis, capping and binding of colloidal gold nanoparticles to proteins, Adv. Nat. Sci: Nanosci. Nanotechnol. 1 (2010) 025009.
[13] A.K. Oyelere, P.C. Chen, X.H. Huang, I.H. El-Sayed, M.A. El-Sayed, Peptide-conjugated gold nanorods for nuclear targeting, Bioconjugate Chem. 18 (2007) 1490–1497.
[14] C.D. Medley, S. Bamrungsap, W.H. Tan, J.E. Smith, Aptamer-conjugated nanoparticles for cancer cell detection, Anal. Chem. 83 (2011) 727–734.
[15] L.L. Yang, H. Mao, Y.A. Wang, Z.H. Cao, X.H. Peng, X.X. Wang, H.W. Duan, C.C. Ni, Q.G. Yuan, G. Adams, M.Q. Smith, W.C. Wood, X.H. Gao, S.M. Nie, Single chain epidermal growth factor receptor antibody conjugated nanoparticles for in vivo tumor targeting and imaging, Small 5 (2009) 235–243.
[16] M. De, P.S. Ghosh, V.M. Rotello, Applications of nanoparticles in biology, Adv. Mater. 20 (2008) 4225–4241.
[17] J.E. Gestwicki, L.E. Strong, L.L. Kiessling, Visualization of single multivalent receptor-ligand complexes by transmission electron microscopy, Angew. Chem. Int. Ed. 39 (2000) 4567–4570.
[18] S. Hakomori, Glycosylation defining cancer malignancy: new wine in an old bottle, Proc. Natl. Acad. Sci. U. S. A. 99 (2002) 10231–10233.
[19] H. Lis, N. Sharon, Lectins: carbohydrate-specific proteins that mediate cellular recognition, Chem. Rev. 98 (1998) 637–674.
[20] R. Sinha, G.J. Kim, S.M. Nie, D.M. Shin, Nanotechnology in cancer therapeutics: bioconjugated nanoparticles for drug delivery, Mol. Cancer Ther. 5 (2006) 1909–1917.
[21] Q.F. Liu, X.Y. Shao, J. Chen, Y.H. Shen, C.C. Feng, X.L. Gao, Y. Zhao, J.W. Li, Q.Z. Zhang, X.G. Jiang, In vivo toxicity and immunogenicity of wheat germ agglutinin conjugated poly (ethylene glycol)-poly(lactic acid) nanoparticles for intranasal delivery to the brain, Toxicol. Appl. Pharmacol. 251 (2011) 79–84.
[22] A. Sharma, S. Sharma, G.K. Khuller, Lectin-functionalized poly (lactide-co-glycolide) nanoparticles as oral/aerosolized antitubercular drug carriers for treatment of tuberculosis, J. Antimicrob. Chemother. 54 (2004) 761–766.
[23] G. Obaid, I. Chambrier, M.J. Cook, D.A. Russell, Targeting the oncofetal Thomsen-Friedenreich disaccharide using jacalin-PEG phthalocyanine gold nanoparticles for photodynamic cancer therapy, Angew. Chem. Int. Ed. 51 (2012) 6158–6162.
[24] R. Sankaranarayanan, K. Sekar, R. Banerjee, V. Sharma, A. Surolia, M. Vijayan, A novel mode of carbohydrate recognition in jacalin, a *Moraceae plant* lectin with a beta-prism fold, Nat. Struct. Biol. 3 (1996) 596–603.
[25] S.K. Mahanta, M.V.K. Sastry, A. Surolia, Topography of the combining region of a Thomsen-Friedenreich-antigen-specific lectin jacalin (*artocarpus-integrifolia* agglutinin) – a thermodynamic and circular-dichroism spectroscopic study, Biochem. J. 265 (1990) 831–840.
[26] A.A. Jeyaprakash, P.G. Rani, G.B. Reddy, S. Banumathi, C. Betzel, K. Sekar, A. Surolia, M. Vijayan, Crystal structure of the jacalin-T-antigen complex and a comparative study of lectin-T-antigen complexes, J. Mol. Biol. 321 (2002) 637–645.

[27] S. Kabir, Jacalin: a jackfruit (*Artocarpus heterophyllus*) seed-derived lectin of versatile applications in immunobiological research, J. Immunol. Methods 212 (1998) 193–211.
[28] X.Y. Shi, T.R. Ganser, K. Sun, L.P. Balogh, J.R. Baker, Characterization of crystalline dendrimer-stabilized gold nanoparticles, Nanotechnology 17 (2006) 1072–1078.
[29] X.O. Liu, M. Atwater, J.H. Wang, Q. Huo, Extinction coefficient of gold nanoparticles with different sizes and different capping ligands, Colloid Surf. B Biointerfaces 58 (2007) 3–7.
[30] D. Gupta, N. Rao, K.D. Puri, K.L. Matta, A. Surolia, Thermodynamic and kinetic-studies on the mechanism of binding of methylumbelliferyl glycosides to jacalin, J. Biol. Chem. 267 (1992) 8909–8918.
[31] J.R. Lakowicz, Principles of Fluorescence Spectroscopy, 2 ed., Plenum Press, New York, 1999.
[32] I. Jelesarov, H.R. Bosshard, Isothermal titration calorimetry and differential scanning calorimetry as complementary tools to investigate the energetics of biomolecular recognition, J. Mol. Recognit. 12 (1999) 3–18.
[33] S. Thobhani, S. Attree, R. Boyd, N. Kumarswami, J. Noble, M. Szymanski, R.A. Porter, Bioconjugation and characterisation of gold colloid-labelled proteins, J. Immunol. Methods 356 (2010) 60–69.
[34] L. Jurgens, A. Nichtl, U. Werner, Electron density imaging of protein films on gold-particle surfaces with transmission electron microscopy, Cytometry 37 (1999) 87–92.
[35] R. Shukla, V. Bansal, M. Chaudhary, A. Basu, R.R. Bhonde, M. Sastry, Biocompatibility of gold nanoparticles and their endocytotic fate inside the cellular compartment: A microscopic overview, Langmuir 21 (2005) 10644–10654.
[36] N. Sreerama, R.W. Woody, Estimation of protein secondary structure from circular dichroism spectra: comparison of CONTIN, SELCON, and CDSSTR methods with an expanded reference set, Anal. Biochem. 287 (2000) 252–260.
[37] M. Mahmoudi, I. Lynch, M.R. Ejtehadi, M.P. Monopoli, F.B. Bombelli, S. Laurent, Protein-nanoparticle interactions: opportunities and challenges, Chem. Rev. 111 (2011) 5610–5637.
[38] A. Barth, Infrared spectroscopy of proteins, Biochim. Biophys. Acta-Bioenerg. 1767 (2007) 1073–1101.
[39] A. Barth, The infrared absorption of amino acid side chains, Prog. Biophys. Mol. Biol. 74 (2000) 141–173.
[40] L. Shang, Y.Z. Wang, J.G. Jiang, S.J. Dong, pH-dependent protein conformational changes in albumin: gold nanoparticle bioconjugates: A spectroscopic study, Langmuir 23 (2007) 2714–2721.
[41] A. Shpigelman, G. Israeli, Y.D. Livney, Thermally-induced protein–polyphenol co-assemblies: beta lactoglobulin-based nanocomplexes as protective nanovehicles for EGCG, Food Hydrocolloids 24 (2010) 735–743.
[42] M. De, C.C. You, S. Srivastava, V.M. Rotello, Biomimetic interactions of proteins with functionalized nanoparticles: a thermodynamic study, J. Am. Chem. Soc. 129 (2007) 10747–10753.
[43] G. Baier, C. Costa, A. Zeller, D. Baumann, C. Sayer, P.H.H. Araujo, V. Mailander, A. Musyanovych, K. Landfester, BSA adsorption on differently charged polystyrene nanoparticles using isothermal titration calorimetry and the influence on cellular uptake, Macromol. Biosci. 11 (2011) 628–638.
[44] M. De, O.R. Miranda, S. Rana, V.M. Rotello, Size and geometry dependent protein-nanoparticle self-assembly, Chem. Commun. (2009) 2157–2159.
[45] K.M. Chen, Y.S. Xu, S. Rana, O.R. Miranda, P.L. Dubin, V.M. Rotello, L.H. Sun, X.H. Guo, Electrostatic selectivity in protein-nanoparticle interactions, Biomacromolecules 12 (2011) 2552–2561.
[46] M. Yagi, A. Camposneto, K. Gollahon, Morphological and biochemical-changes in a hematopoietic-cell line induced by jacalin, a lectin derived from *artocarpus-integrifolia*, Biochem. Biophys. Res. Commun. 209 (1995) 263–270.
[47] A.M. Wu, J.H. Wu, L.H. Lin, S.H. Lin, J.H. Liu, Binding profile of Artocarpus integrifolia agglutinin (Jacalin), Life Sci. 72 (2003) 2285–2302.
[48] G. Maiorano, S. Sabella, B. Sorce, V. Brunetti, M.A. Malvindi, R. Cingolani, P.P. Pompa, Effects of cell culture media on the dynamic formation of protein-nanoparticle complexes and influence on the cellular response, ACS Nano 4 (2010) 7481–7491.
[49] U. Chatterjee, P.P. Bose, S. Dey, T.P. Singh, B.P. Chatterjee, Antiproliferative effect of T/Tn specific Artocarpus lakoocha agglutinin (ALA) on human leukemic cells (Jurkat, U937, K562) and their imaging by QD-ALA nanoconjugate, Glycoconjugate J. 25 (2008) 741–752.